Control of a nonlinear ice cream crystallization process

Céline Casenave, Denis Dochain, Graciela Alvarez, Marcela Arellano, Hayat Benkhelifa, Denis Leducq

HAL Id: hal-00859552
https://hal.inria.fr/hal-00859552

Submitted on 17 Sep 2014

Control of a nonlinear ice cream crystallization process [⋆]

Céline Casenave [∗] **Denis Dochain** [∗∗] **Graciela Alvarez** [∗∗∗]
Marcela Arellano [∗∗∗] **Hayat Benkhelifa** [∗∗∗∗] **Denis Leducq** [∗∗∗]

[∗] *MODEMIC project-team, INRA/INRIA, 2 place Pierre Viala, 34060
Montpellier, France (e-mail: celine.casenave@supagro.inra.fr).*
[∗∗] *ICTEAM, UCL, 4 avenue Georges Lemaître 1348 Louvain-la-neuve,
Belgium (e-mail: denis.dochain@uclouvain.be)*
[∗∗∗] *IRSTEA, 1 rue Pierre-Gilles de Gennes, 92160 Antony, France
(e-mail: {graciela.alvarez, marcela.arellano, denis.leducq}@irstea.fr)*
[∗∗∗∗] *AgroParisTech , UMR n° 1145 Ingénierie-Procédés-Aliments, 16
rue Claude Bernard, 75231 Paris Cedex 05, France. (e-mail:
hayat.benkhelifa@agroparistech.fr)*

Abstract: In the ice cream industry, the type of final desired product (large cartons (sqrounds) or ice creams on a stick) determine the viscosity at which the ice cream has to be produced. One of the objectives of the ice cream crystallization processes is therefore to produce an ice cream of specified viscosity. In this paper, a nonlinear control strategy is proposed for the control of the viscosity of the ice cream in a continuous crystallizer. It has been designed on the basis of a reduced order model obtained by application of the method of moments, on a population balance equation describing the evolution of the crystal size distribution. The control strategy is based on a linearizing control law coupled with a Smith predictor to account for the measurement delay. It has been validated on a pilot plant located at IRSTEA (Antony, France).

1. INTRODUCTION

Crystallization is prominent in the process industry nowadays, in particular in the micro-electronic pharmaceutical and food industries (**?**). In crystallization processes, an important challenge is to control the properties of the final product. These properties (as for example in the pharmaceutical industry, the bioavailability and the shelf-life) are often directly linked to the characteristics of the crystals. In particular, the product efficiency and quality depend on the shape of the crystals and on the one of the crystal size distribution (CSD). The control of the shape of the CSD has therefore appeared essential in crystallization processes and has lead to the development of numerous control strategies both in batch and continuous crystallizers (**???**). Some of the properties of the product do not depend on the whole CSD, but only on some related quantities, as for example the moments of the CSD, the control of which has also been studied in several papers (**??**).

In ice cream crystallization, it is well known that the quality of the product, that is the hardness and the texture of the ice cream, depends on the ice CSD. Indeed, an ice cream with a narrow ice CSD and a small mean ice crystals size is smoother and more palatable. But it can also be interesting, in a production point of view, to control other properties of the ice cream, as its viscosity. Indeed, the ice cream market is characterized by a variety of products that can be classified in particular in term of their final packaging. Each type of final product is characterized by a specified viscosity: for instance a lower viscosity is required for large carton packaging than for cones. One of the objectives of ice cream crystallization processes is therefore to produce an ice cream of specified viscosity.

The viscosity of the ice cream can be expressed as a function of the ice temperature and the third moment of the ice CSD. As a consequence, it is not necessary to control the shape of the CSD itself: we only need to control the third moment. A model that describes the evolution of this moment can be achieved from a population balance equation (PBE) (**?**) describing the evolution of the CSD. By applying the method of moments, the PBE is transformed in a set of ordinary differential equations (ODEs). This system is coupled with an energy balance equation, and an equation of the dynamic of the compressor of the crystallizer. As the first four moment equations are independent of the ones of lower order, and as the energy balance equation only involves moments of order 3 or less, the system we consider is reduced to a set of 6 ODEs.

In this paper, a nonlinear control strategy is proposed for the control of the viscosity of the ice cream in a continuous crystallizer. It is based on a linearizing control law coupled with a Smith predictor to account for the measurement delay, as in the general approach proposed in **?** for the control of particulate processes. The control strategy has been validated on a pilot plant located at IRSTEA (Antony, France).

This work was conducted as a part of the European CAFE project (Computer-Aided Food processes for control Engineering) in which four case studies are considered among them the one of the ice crystallization process.

The paper is organized as follows. In section 2 the pilot plant is described. Then, the reduced order model is given is section 3 and compared to experimental data. In section 4, the choice of the output to be controlled and the one of the control input are discussed. Then the design of the control law is presented in section 5. Finally, the control strategy is validated on the experimental pilot plant in section 6.

2. PROCESS DESCRIPTION

2.1 Pilot plant

The pilot plant is located at IRSTEA Antony (France). The ice cream crystallizer is a 0.40 meter long cylindric scraped surface heat exchanger, with inner diameter of 0.05 meter. The mix sorbet, which is mainly composed of sugar, gum and water, is first put in a mix storage tank which is refrigerated at a temperature T_0 of $5°C$. The mix sorbet is then conducted in the crystallizer by a piston pump with a mass flow rate denoted m_{fr}. Within the vessel jacket of the crystallizer, a refrigerant fluid, whose temperature T_e is called the evaporation temperature, is continually vaporizing to cool down the mix sorbet. When the temperature of the mix sorbet gets smaller than a threshold temperature called the saturation temperature, and denoted T_{sat}, the crystallization occurs. Some ice crystals appear at the inner wall of the cylinder and are scraped by two scraper blades which turn with a rotation speed denoted N_{scrap} and so mix the ice.

The evaporation temperature T_e can be varied from $-10°C$ to $-25°C$ through a compressor with rotation speed V_{comp}. The dasher rotation speed can be varied from 300 to 1000 rpm and the mix flow rate m_{fr} from 20 to 100 kg.h^{-1}.
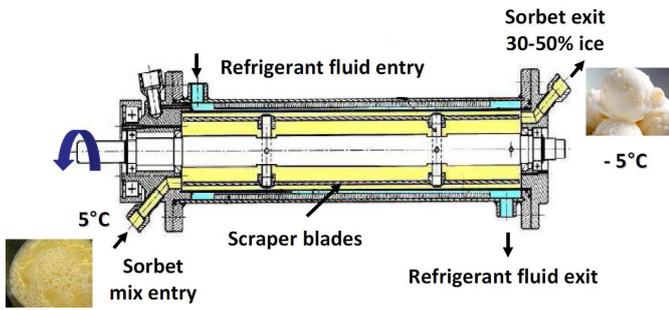

Fig. 1. Scheme of the freezer

2.2 Available measurements

Two variables are accessible for on-line measurement : the outlet temperature T of the ice cream and the evaporation temperature T_e. The temperature T is measured at some distance of the reactor outlet, and can be reasonably considered to be equal (at this measurement point) to the saturation temperature T_{sat}. Indeed the temperature inside the freezer has to be lower than the saturation

temperature so that the crystallization can proceed. When the ice leaves the reactor through a non refrigerated pipe, the temperature of the ice increases to reach the saturation temperature value.

Note that the location of the measurement point at some distance of the reactor generates measurement delay. By denoting T_{sat}^{m} the temperature measurement, we have :

$$T_{sat}^{m}(t) = T_{sat}(t - d) + \varepsilon_T \qquad (1)$$

where T_{sat} is the saturation temperature of the ice at the outlet of the freezer, d is the measurement delay and ε_T is the measurement error.

3. MODEL DESCRIPTION AND VALIDATION

3.1 Model of the process

The model considered here is a set of 6 energy and mass balance equations; it is written:

$$\frac{dM_0}{dt} = -DM_0 + N + BM_1 \qquad (2)$$

$$\frac{dM_1}{dt} = -DM_1 + GM_0 + NL_c + c_1BM_2 \qquad (3)$$

$$\frac{dM_2}{dt} = -DM_2 + 2GM_1 + NL_c^2 + c_2BM_3 \qquad (4)$$

$$\frac{dM_3}{dt} = -DM_3 + 3GM_2 + NL_c^3 \qquad (5)$$

$$\frac{dT}{dt} = D(T_0 - T) + K_2(T_e - T) + \mu N_{scrap}^2 K_3 \\ + K_1(3GM_2 + NL_c^3) \qquad (6)$$

$$\frac{dT_e}{dt} = -\frac{1}{\tau_c}T_e + \frac{1}{\tau_c}G^c, \qquad (7)$$

where:

- M_i is the ith order moment defined by:

$$M_i = \int_0^\infty L^i \psi(t, L)dL, \qquad (8)$$

with L the crystal size variable and $\psi(t,.)$ the crystal size distribution at time t, at the outlet of the freezer;
- T (respectively T_0) is the temperature of the ice at the outlet (respectively at the inlet) of the freezer;
- T_e is the evaporation temperature;
- D is the dilution rate, which is proportional to the inlet mass flow rate m_{fr} ($D = \frac{m_{fr}}{\rho V}$, with ρ and V the mix density and the crystallizer volume, respectively);
- N_{scrap} is the dasher rotation speed;
- V_{comp} is the compressor rotation speed;
- $\mu = \mu(M_3, T)$ is the viscosity of the ice, which is assumed to depend only on M_3 and T;
- $T_{sat} = T_{sat}(M_3)$ is the saturation temperature, that is the threshold temperature below which the ice crystallizes (on the contrary, the ice is melting behind this value). It is assumed to depend only on M_3;
- G and N are the growth and nucleation rates, respectively, expressed by [1] (?):

$$G(M_3, T) = \beta(T_{sat}(M_3) - T), \qquad (9)$$

$$N(M_3, T_e) = \alpha S(T_{sat}(M_3) - T_e)^2, \qquad (10)$$

where α, β are some kinetic parameters and S is a constant depending on the size of the freezer;

[1] Only heterogeneous nucleation at the freezer wall is considered.

- B is a breakage constant, assumed to be proportional to N_{scrap}: $B = \epsilon\, N_{\mathrm{scrap}}$;
- $G^c = G^c(V_{\mathrm{comp}}, \mathrm{m_{fr}}, N_{\mathrm{scrap}})$ is the nonlinear gain of the T_e dynamic; it is assumed to depend on V_{comp}, $\mathrm{m_{fr}}$ and N_{scrap}.
- K_1, K_2 and K_3 are some constant parameters depending on the ice and the device, τ_c is the T_e dynamic time constant, $c_1 = 2^{\frac{2}{3}} - 1$ and $c_2 = 2^{\frac{1}{3}} - 1$.

Remark 1. M_0, M_1, M_2 and M_3 represent the number of particles, the sum of characteristic lengths and the images of the total area and volume of the crystals per cubic meter at the outlet of the freezer respectively. Their respective units are $[m^{-3}]$, $[m^{-2}]$, $[m^{-1}]$ and $[-]$.

The first part of the model (equations (2) to (6)) has been developed by research teams of AgroParisTech and IRSTEA Antony (France) and has been validated, at equilibrium, on experimental data obtained from the pilot plant; it is described in **??**. This model has been obtained by reduction of a more complex one, composed of a population balance equation (PBE) of the crystal size distribution coupled with an energy balance equation. The PBE considers transport, crystal growth, nucleation and breakage. Under some hypotheses on the breakage term [2] and by application of the method of moments [3], the PBE has been transformed in a closed set of 5 ordinary differential equations.
In **?**, the steady-states analysis of this part of the model has been performed.

As for the equation of T_e, it describes the dynamic of the compressor which behaves like a first order system with a nonlinear gain (see **?**).

3.2 Parameter identification

Model (2-7) includes several parameters whose values have to be adjusted. Concerning the 5 first equations of the model, an initial parameter values set is given in **???**. From this parameters set, a sensitivity analysis has been performed: the 2 parameters K_2 and K_3 have been identified as the more sensitive parameters of these equations. Then the values of these parameters have been optimized in a least squares sense to fit the data at best: a simplex method was used to minimize the distance between experimental data and simulated trajectories.

The function G_c of the equation of T_e has been identified from experimental data at equilibrium. The time constant τ_c has been optimized in a least squares sense from experimental data.

In figure 2, some trajectories obtained by simulation of the model with the optimized parameter values set are compared with some experimental data. The first one (in solid line) is obtained by simulation of the full system (2-6), whereas the second one (in dotted line) is obtained by simulation of the following reduced order model:

$$\frac{dM_3}{dt} = -DM_3 + 3G\frac{M_3}{L_{\mathrm{mean}}} + NL_c^3 \qquad (11)$$

$$\frac{dT}{dt} = D\left(T_0 - T\right) + K_2\left(T_e - T\right) + \mu N_{\mathrm{scrap}}^2 K_3 \qquad (12)$$

$$+ K_1\left(3G\frac{M_3}{L_{\mathrm{mean}}} + NL_c^3\right),$$

in which the parameter L_{mean} has also been identified. This model has been obtained from the full model (2-6) in which M_2 has been approximated from the value of M_3 by:

$$M_2 \simeq \frac{1}{L_{mean}} \int_0^\infty L^3 \psi(t,L)dL = \frac{1}{L_{mean}}M_3, \qquad (13)$$

where L_{mean} stands for the mean value of L. The parameters and functions used for the simulations are given here after.

The expression of T_{sat} (in $[°C]$) is given by (see **?**):
$T_{\mathrm{sat}}(M_3) = -7.693\omega + 8.64\omega^2 - 70.053\omega^3$ with
$\omega = \dfrac{\omega_0}{1 - \rho\phi_i}\,[-]$, $\phi_i = \dfrac{\pi}{6}M_3\,[-]$, $\omega_0 = 0.25\,[-]$, $\rho = 0.9091\,[-]$.

The expression of the viscosity (in $[Pa.s]$) has been obtained empirically; it is given by (see **??**) :
$$\mu(M_3, T) = \mu_{\mathrm{mix}}\left(1 + 2.5\,\phi_i + 10.05\,\phi_i^2 + 0.9555\,e^{16.6\,\phi_i}\right)$$
with $\mu_{\mathrm{mix}} = 39.02\,10^{-9} \times \gamma_{\mathrm{pav}}^{0.600-1}e^{\frac{2242.38}{T+273}} \times (100\,\omega)^{2.557}$,
where $\gamma_{\mathrm{pav}} = 12.57 \times N_{\mathrm{scrap}}[s^{-1}]$.
The other parameters are given hereafter [4] :
$D = 1.813\,10^{-7} \times \mathrm{m_{fr}}\,[s^{-1}]$; $N_{\mathrm{scrap}} = 12.5\,[\mathrm{r.s^{-1}}]$; $\beta = 5\,10^{-7}\,[\mathrm{m.s^{-1}.K^{-1}}]$; $\alpha S = 1.355\,10^{11}\,[\mathrm{m^{-3}.s^{-1}.K^{-2}}]$; $\epsilon = 20\,[\mathrm{m^{-1}}]$; $L_c = 5\,10^{-6}\,[\mathrm{m}]$; $L_{\mathrm{mean}} = 1.676\,10^{-5}\,[\mathrm{m}]$; $T_0 = 5\,[°C]$; $d = 50[\mathrm{s}]$; $K_1 = 44.61\,[K]$; $K_2 = 0.0775\,[s^{-1}]$; $K_3 = 5.278\,10^{-6}\,[-]$.

For the equation of T_e, the parameter τ_c is taken equal to :
$$\tau_c = 30\,[s], \qquad (14)$$
and the function G^c is given by:
$$G^c(V_{\mathrm{comp}}, \mathrm{m_{fr}}, N_{\mathrm{scrap}}) = -6.855$$
$$+ 2.185\,10^2\,\mathrm{m_{fr}} - 1.346\,10^{-1}\,N_{\mathrm{scrap}} - 1.122V_{\mathrm{comp}}$$
$$- 2.770\,10^3\,\mathrm{m_{fr}}^2 + 9.562\,10^{-3}N_{\mathrm{scrap}}^2 + 1.987\,10^{-2}\,V_{\mathrm{comp}}^2.$$

4. PRACTICAL SELECTION OF THE CONTROL VARIABLES

4.1 Controlled output

Recall that the objective is to control the viscosity μ of the product at the outlet of the freezer, or more precisely at the measurement point, located a bit further than the outlet of the freezer. At this measurement point, the temperature of the ice is close to the saturation temperature $T_{\mathrm{sat}}(M_3)$. As μ is a function of the two variables T and M_3, we have, at the measurement point :
$$\mu = \mu(M_3, T_{\mathrm{sat}}(M_3)) = \widetilde{\mu}(M_3). \qquad (15)$$
Therefore, the control of the product viscosity at the measurement point can be achieved via the control of the variable M_3 or of the saturation temperature $T_{\mathrm{sat}}(M_3)$. Because a measurement of the saturation temperature is

---

[2] We assume that a particle of size L' is broken into two particles of the same length L. The volume of ice is considered unchanged by the fragmentation and a spherical shape is assumed (as in **?**)

[3] The method of moments consists in multiplying the population balance equation by L^j, and then in integrating it from $L = 0$ to $L = \infty$.

[4] r stands for the rotations, and K for the Kelvin degrees. $\mathrm{m_{fr}}$ is given in $\mathrm{kg.s^{-1}}$.

available (which is not the case for M_3), T_{sat} is chosen as the output to be controlled; we denote:

$$y = T_{\text{sat}}(M_3) \qquad (16)$$

and $y^* = T_{\text{sat}}^*$ the desired saturation temperature corresponding to a unique given value of the desired viscosity.

4.2 Control input selection

Three control inputs can be used to control the viscosity μ: the compressor rotation speed V_{comp} (linked to the evaporation temperature T_e), the mass flow rate m_{fr} (linked to the dilution rate D), and the dasher rotation speed N_{scrap}.

First of all, the absence of correlation between μ and N_{scrap} has been exhibited experimentally. This lack of correlation is also a feature of the dynamical model (2)-(6). Indeed it has been assumed that when it breaks, a crystal divides itself in two crystals of same volume and that the total volume is conserved. As a consequence and as M_3 represents the total volume of the crystals per cubic meter, the breakage (and so N_{scrap}) does not influence the value of M_3 (and so of $\widetilde{\mu}(M_3)$) a lot.
This can be seen in Table 1, where the influence of each of the possible control inputs on the value M_3^{eq} of M_3 at equilibrium has been evaluated in numerical simulations.

Secondly m_{fr} is linked to the productivity of the system: it is so considered fixed in the sequel.

Finally, only V_{comp} is used to control T_{sat}. More precisely, a cascade control is used with two control loops: a primary

T_e	-20	**-18**	-16	-14	-12
M_3^{eq}	0.4114	**0.3524**	0.2898	0.2245	0.1576

	N_{scrap}	250	500	**750**	1000	
	M_3^{eq}	0.3574	0.3552	**0.3524**	0.3490	

m_{fr}	25	35	45	55	65	**75**
M_3^{eq}	0.6678	0.6190	0.5573	0.4864	0.4157	**0.3524**

Table 1. Sensitivity of the output M_3 at equilibrium to the different control inputs. In each table, only one control input is tested and only its value is changed; the others quantities are fixed at the following values: $T_e = -18\,[°\text{C}]$, $N_{\text{scrap}} = 750\,[\text{rpm}]$, $m_{\text{fr}} = 75\,[\text{kg.h}^{-1}]$.

loop to control T_{sat} with T_e, and a secondary loop to control T_e with V_{comp}.

Let us denote in the following :

$$u_1 = T_e,\ u_2 = V_{\text{comp}}. \qquad (17)$$

5. DESIGN OF THE CONTROL LAWS

5.1 Linearizing control strategies

In order to take advantage of the system nonlinearities, a linearizing control law is considered to control T_e with V_{comp}. The T_e equation has a relative degree equal to 1, and the function G^c can be decomposed as follows :

$$G^c(V_{\text{comp}}, D, N_{scrap}) = G_1^c(V_{\text{comp}}) + G_2^c(D, N_{scrap}),$$

with G_1^c an invertible function (invertible on the interval of admissible physical values of V_{comp}). The control law is therefore written as follows :

$$u_2 = (G_1^c)^{-1}\left(\tau_c v_2 + T_e - G_2^c(D, N_{scrap})\right) \qquad (18)$$

with v_2 of the PID form $(K_{p,2},\ K_{d,2},\ K_{i,2} \in \mathbb{R})$:

$$v_2 = K_{p,2}\left(T_e^* - T_e\right) + K_{d,2}\frac{dT_e}{dt} + K_{i,2}\int_0^t \left(T_e^*(\tau) - T_e(\tau)\right) d\tau.$$

Similarly a linearizing control law is also considered to control T_{sat} with T_e. Note that formally the equation of M_3 has a relative degree (with respect to $u_1 = T_e$) equal to 1, because N depends on u_1. However, the term depending on N has a very low sensitivity due to the very small value of L_c (the size at which the crystals are formed by nucleation) and can therefore be neglected. We indeed have the following result.

Proposition 2. By denoting $X = (M_0, M_1, M_2, M_3, T)^T$ the vector of the first five state variables, and f_{M_2}, f_{M_3}, f_T and $f_T^{u_1}$ the functions such that:

$$\frac{dM_2}{dt} = f_{M_2}(X) + NL_c^2,\ \frac{dM_3}{dt} = f_{M_3}(X) + NL_c^3$$

$$\text{and } \frac{dT}{dt} = f_T(X) + f_T^{u_1}(X)u_1 + K_1 NL_c^3,$$

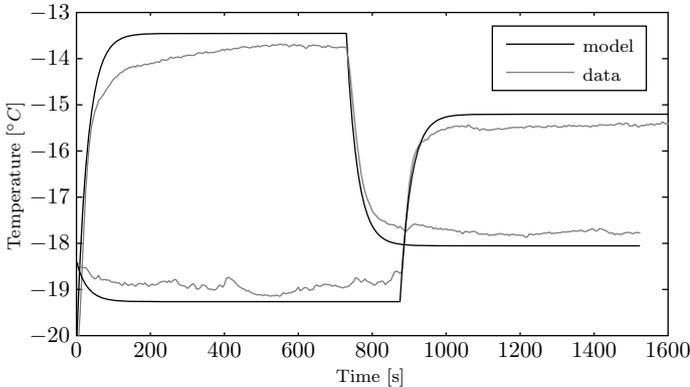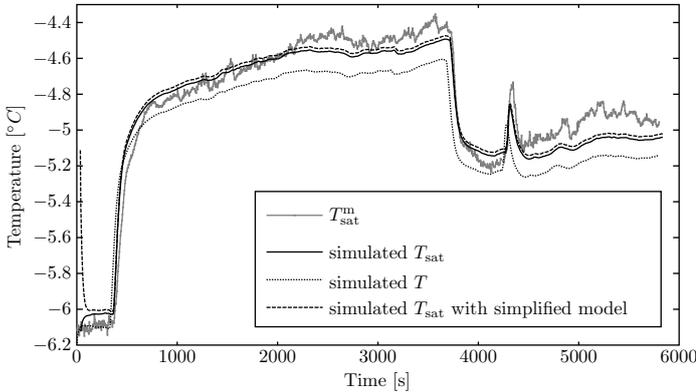the equation of $T_{\text{sat}}(M_3)$ is written [5] :

Fig. 2. Comparison between experimental data and simulated trajectories. Top: saturation temperature T_{sat}. Bottom: evaporation temperature T_e.

---

[5] In the sequel, and for simplicity, we will denote $G = G(M_3, T)$, $N = N(M_3, u_1)$, $\mu = \mu(M_3, T)$, $T_{sat} = T_{sat}(M_3)$, $T_{sat}' = T_{sat}'(M_3)$, $T_{sat}'' = T_{sat}''(M_3)$ and $T_0 = \frac{U_{in}}{K_0}$.

T_e	$N(.,x)$	M_3^{eq}
-18	N(.,-18)	0.3524
-12	N(.,-12)	0.1576
-18	N(.,-12)	0.3440
-12	N(.,-18)	0.1642

Table 2. Sensitivity of the output value M_3^{eq} of M_3 at equilibrium to the variation of T_e in N and $K_2(u_1 - T)$ independently. For the simulations, we have taken: $N_{\mathrm{scrap}} = 750\,\mathrm{rpm}$, $\mathrm{m_{fr}} = 75\,\mathrm{kg.h^{-1}}$

$$\frac{d^2 y}{dt^2} = a(X)u_1 + b(X) + o(L_c)$$

with: $a(X) = 3M_2 f_T^{u_1}(X) \frac{\partial G}{\partial T} T'_{sat}$

$$b(X) = (f_{M_3}(X))^2 T''_{\mathrm{sat}} + \left[\left(-D + 3\frac{\partial G}{\partial M_3} M_2 \right) f_{M_3}(X) \right.$$

$$\left. + 3\frac{\partial G}{\partial T} f_T(X) M_2 + 3G f_{M_2}(X) \right] T'_{sat}.$$

Proof. The result is obtained by simple computations from the fact that $NL_c^j = o(L_c^{j-1})$, $j = 2:3$ and because:

$$\frac{d^2 y}{dt^2} = T''_{\mathrm{sat}} \left(\frac{dM_3}{dt} \right)^2 + T'_{\mathrm{sat}} \left(-D\frac{dM_3}{dt} + 3G\frac{dM_2}{dt} \right.$$

$$\left. + 3\frac{\partial G}{\partial M_3} \frac{dM_3}{dt} M_2 + 3\frac{\partial G}{\partial T} \frac{dT}{dt} M_2 + \frac{dN}{dt} L_c^3 \right).$$

$$\square$$

Let us now analyze further the system dynamics and check whether the term NL_c^3 can really be neglected in the equation of M_3. There are only two u_1-dependent quantities in the model: $N(M_3, u_1)$ which is present in each of the first 5 state equations, and $K_2(u_1 - T)$ in the equation of T. The influence of these quantities on the value M_3^{eq} of M_3 at equilibrium has been evaluated in numerical simulations. The results are given in table 2. It shows that the sensitivity of M_3^{eq} to T_e is essentially due to the term $K_2(u_1 - T)$ of the equation of T. In other words, the term $N(M_3, u_1)L_c^3$ can be neglected in the equation of M_3 and the linearizing control law u_1 is therefore written:

$$u_1 = -\frac{b(X)}{a(X)} + \frac{v_1}{a(X)}, \qquad (19)$$

with v_1 of the form:

$$v_1 = K_{p,1}(y^* - y) + K_{d,1}\frac{dy}{dt} + K_{i,1}\int_0^t (y^*(\tau) - y(\tau))\,d\tau. \qquad (20)$$

5.2 Simplifications of the control law expressions

In accordance with the experimental evidence, it can be assumed that, at each time instant, the u_1-independent part of the instantaneous time variation of $\frac{dy}{dt}$ (that is the quantity $b(X)$) is essentially due to the u_1-independent part of the instantaneous time variation of T (that is $f_T(X)$). In other words it simply means, that, at each time instant, if the input u_1 is suddenly put at 0, then the variation of the saturation temperature will be modified for the most part because of the variation of the temperature T of the ice (and not because of the one of the moments which are not instantaneously affected by the variation of u_1). This assumption can be expressed in the following way :

$$b(X) \simeq 3\frac{\partial G}{\partial T} f_T(X) T'_{sat} M_2. \qquad (21)$$

Note that this approximation has been verified in numerical simulations, for the identified parameter values set given before and for different realistic operating conditions. The numerical value of the neglected part of $b(X)$ was 100 times smaller than the rest.

Under this assumption, and after computations, the control law u_1 given by (19) can then be written as follows :

$$u_1 \simeq \frac{-D(T_0 - T) + K_2 T - \mu N_{\mathrm{scrap}}^2 K_3 - 3K_1 G M_2}{K_2} \qquad (22)$$

$$- \frac{v_1}{3\beta M_2 K_2 T'_{sat}}, \quad \text{with } v_1 \text{ given by } (20).$$

5.3 Estimation of the unknown quantities

To apply the control laws, the values of the dynamic quantities T_e, M_2, M_3, T and $\frac{dy}{dt}$ are needed. However, only the saturation temperature and the evaporation temperature are measured. To estimate the other quantities, a state-observer could be used. However, state-observers can be pretty difficult to adjust and to initialize, especially when the system is of great dimension, and when the model is not accurate enough. The unknown quantities of the control laws are estimated here in a different way:

- As explained before, the measurement $T_{\mathrm{sat}}^{\mathrm{m}}$ of T_{sat} is delayed. To compensate the delay, a Smith predictor based on the simplified model (11,12) is used as in **?**.
- From the measurement $T_{\mathrm{sat}}^{\mathrm{m}}$ of T_{sat}, we can deduce an approximate value of M_3. Indeed, the function T_{sat} only depends on M_3 and is bijective[6]. An estimate M_3^{m} of M_3 is so obtained by:

$$M_3^{\mathrm{m}} = T_{\mathrm{sat}}^{-1}(T_{\mathrm{sat}}^{\mathrm{m}}). \qquad (23)$$

- For M_2, we use the same approximation than the one used for the reduced model given in section 3.2, that is :

$$M_2 \simeq \frac{1}{L_{\mathrm{mean}}} M_3, \qquad (24)$$

  with L_{mean} the mean crystal size.
- The value of T at the outlet of the freezer stays close to the one of T_{sat} (see figure 2). The value of G is therefore small and the G-dependent term can be neglected.
- An estimate of $\frac{dy}{dt}$ is deduced from the model and the fact that G and L_c-dependent terms can be neglected:
  $\frac{dy}{dt} = -DM_3 T'_{\mathrm{sat}}$.

Under these assumptions, the control law is finally given by :

$$u_1 \simeq -\frac{D(T_0 - T) - K_2 T + \mu N_{\mathrm{scrap}}^2 K_3}{K_2} - \frac{L_{mean}}{3\beta M_3 K_2 T'_{\mathrm{sat}}} v_1,$$

with v_1 given by:

$$v_1 = K_{p,1}(y^* - y) - K_{d,1} DM_3 T'_{\mathrm{sat}} + K_{i,1}\int_0^t (y^*(\tau) - y(\tau))\,d\tau.$$

Remark 3. The initialization of the integral term will be chosen such that the value of the control $u_1 = T_e$ will be equal to the one just before the control law is applied.

---

[6] More precisely, its restriction to the interval $[0, \frac{6}{\rho\pi}[$ of admissible physical values of M_3 is bijective.

6. VALIDATION ON THE EXPERIMENTAL PROCESS

The control laws u_1 and u_2 have been tested and validated first on numerical simulations, and then on the experimental pilot plant described in section 2. Some experimental results [7] are presented in figure 3. The mass flow rate m_{fr} was taken equal to $25\,\mathrm{kg.h^{-1}}$ and the scraper rotation speed N_{scrap} was equal to $655\,[\mathrm{rpm}]$, that is $10.92\,[\mathrm{r.s^{-1}}]$. The values of the control law parameters used for this experiment are given here after:

$$K_{p,1} = 4.375\,10^{-2};\ K_{d,1} = -4.125\,10^{-1};\ K_{i,1} = 1.125\,10^{-3};$$
$$K_{p,2} = 6\,10^{-2};\ K_{d,2} = 0;\ K_{i,2} = 9\,10^{-4}.$$

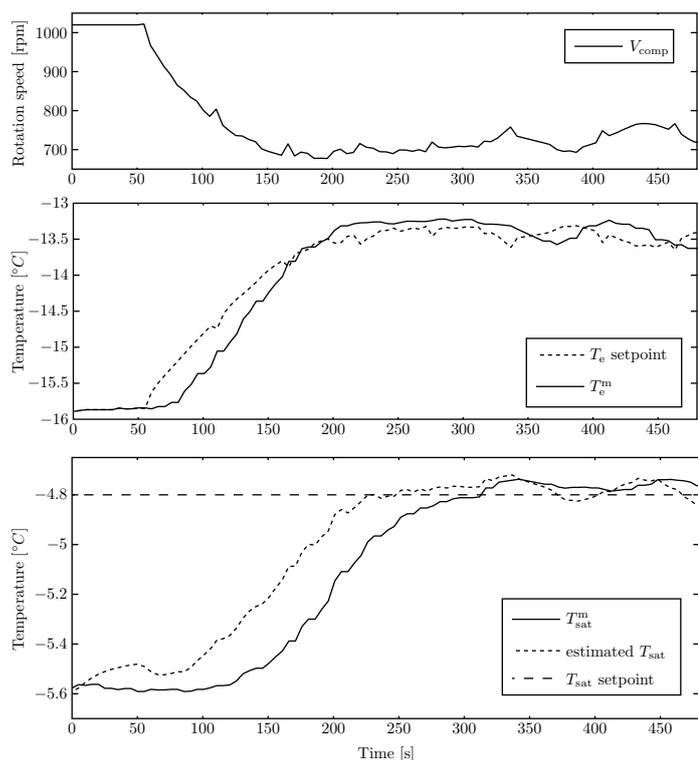On the first graph (top of the figure), the compressor

Fig. 3. Experimental results obtained by application of the control laws u_1 and u_2 on the pilot plant. Top: compressor rotation speed. Center: evaporation temperature setpoint and measurement. Bottom: saturation temperature setpoint, measurement and estimation (with the Smith predictor).

rotation speed is given. In the second graph (center of the figure), the evaporation temperature setpoint computed by the primary loop is given and compared with the measurements which well follow the setpoint curve. Finally, in the third graph (bottom of the figure), the saturation temperature setpoint, measurement and estimation are given. The estimation is the one obtained by the Smith predictor, in which the measurement delay has been compensated. As expected, the estimations curve is shifted in the time domain in comparison with the measurements curve. As for the T_{sat} setpoint, the system manages to reach it and stay close to it.

---

[7] The control laws were only applied to the system for time $t > 50\,[s]$.

7. CONCLUSION

In this paper, a nonlinear cascade control strategy is proposed for the control of the ice cream viscosity at the outlet of a continuous crystallizer. The model considered is highly nonlinear because deduced from the modeling of the ice cream crystallization mechanism which is achieved by a population balance equation. Moreover, only two on-line measurements are available for the control and one of them is delayed. A linearizing control law coupled with a Smith predictor has so been designed. It has been validated first on numerical simulation and then on an experimental process. The next step will now consist in adding an on-line estimation of uncertain parameters, because some of them can vary from one experiment to another, or even during the same experiment.

REFERENCES

C. Antoniades and P. D. Christofides. Feedback control of nonlinear differential difference equation systems. *Chemical engineering science*, 54(23):5677–5709, 1999.

H. Benkhelifa, A. Haddad Amamou, G. Alvarez, and D. Flick. Modelling fluid flow, heat transfer and crystallization in a scraped surface heat exchanger. *Acta Horticulturae (ISHS)*, 802:163–170, 2008.

H. Benkhelifa, M. Arellano, G. Alvarez, and D. Flick. Ice crystals nucleation, growth and breakage modelling in a scraped surface heat exchanger. In *11th International Congress on Engineering and Food (ICEF)*, Athens, Greece, May 2011.

C. Casenave, D. Dochain, G. Alvarez, H. Benkhelifa, D. Flick, and D. Leducq. Steady-state and stability analysis of a population balance based nonlinear ice cream crystallization model. In *American Control Conference (ACC)*, Montréal (Canada), 27-29 june 2012.

T. Chiu and P. D. Christofides. Nonlinear control of particulate processes. *AIChE Journal*, 45(6):1279–1297, 1999.

KLK Cook and RW Hartel. Mechanisms of ice crystallization in ice cream production. *Comprehensive Reviews in Food Science and Food Safety*, 9(2):213–222, 2010.

C.B.B. Costa, M.R.W. Maciel, and R.M. Filho. Considerations on the crystallization modeling: Population balance solution. *Computers & chemical engineering*, 31 (3):206–218, 2007.

J.-E. Gonzalez. *Contribution au contrôle par la modélisation d'un procédé de cristallisation en continu.* PhD thesis, Agroparistech, p 154, 2012.

C. Y. Ma and X. Z. Wang. Closed-loop control of crystal shape in cooling crystallization of l-glutamic acid. *Journal of Process Control*, 22(1):72–81, 2011.

N. V. Mantzaris and P. Daoutidis. Cell population balance modeling and control in continuous bioreactors. *Journal of Process Control*, 14(7):775–784, 2004.

Z. K. Nagy. A population balance model approach for crystallization product engineering via distribution shaping control. *Computer Aided Chemical Engineering*, 25:139–144, 2008.

U. Vollmer and J. Raisch. Control of batch crystallization - A system inversion approach. *Chemical Engineering and Processing: Process Intensification*, 45(10):874–885, 2006.